引用格式：石慧, 谢天成, 刘子亮, 等. 碎裂煤中煤粉运移对孔渗影响的数值模拟研究[J]. 油气藏评价与开发, 2025, 15(6): 1025-1033.
SHI Hui, XIE Tiancheng, LIU Ziliang, et al. Numerical simulation study on influence of coal fines migration on porosity and permeability in cataclastic coal[J]. Petroleum Reservoir Evaluation and Development, 2025, 15(6): 1025-1033.
DOI: 10.13809/j.cnki.cn32-1825/te.2025.06.008

碎裂煤中煤粉运移对孔渗影响的数值模拟研究

石 慧[1], 谢天成[1], 刘子亮[1], 蒋志坤[1], 魏迎春[1,2]
（1.中国矿业大学（北京）地球科学与测绘工程学院，北京 100083；2.中国矿业大学（北京）煤炭精细勘探与智能开发全国重点实验室，北京 100083）

摘要：在煤层气排采过程中，储层中煤粉会发生运移，可能造成孔隙和喉道堵塞，导致渗透率下降，从而影响煤层气的产量。为了探究煤粉运移对碎裂煤储层孔渗的影响，建立了煤粉在孔喉通道内的运移—沉降数值模型，基于python（高级程序设计语言）编写了煤粉运移的数值模拟程序，模拟了煤粉在碎裂煤基质孔隙网络中的运移，探讨了煤粉运移过程中的碎裂煤储层孔渗变化规律以及煤粉运移对孔渗的影响。数值模拟结果表明：压差和煤粉粒度是影响储层孔渗的2个关键因素。模拟初始阶段，煤粉运移引起储层渗透率迅速降低，不同粒径煤粉颗粒运移、沉降和排出进一步受到压差的影响，煤粉粒度越大，在低压差、低流速条件下越难以启动运移，而在压差较大流速较高的情况下，则会发生运移。对比小粒径煤粉，大粒径煤粉颗粒更加容易堵塞有效孔隙，导致渗透率迅速下降。压差增加会使煤粉沉积位置向出口端转移，导致煤粉沉降范围变大。在煤粉粒径小于喉道半径的条件下，驱替压力存在一个阈值，当小于这个阈值时，渗透率的下降速度随着驱替压力的增大而增大；当大于这个阈值时，渗透率的下降速度会随着驱替压力的增大而降低。将数值模拟实验数据与关于煤粉运移的物理模拟实验结果相结合表明：模型的数值模拟结果与物理模拟实验中的煤粉运移过程中碎裂煤的渗透率变化和煤粉产出沉降情况一致。

关键词：煤层气；碎裂煤；煤粉运移；孔渗；煤粉粒径；数值模拟
中图分类号：TE357　　**文献标识码**：A

Numerical simulation study on influence of coal fines migration on porosity and permeability in cataclastic coal

SHI Hui[1], XIE Tiancheng[1], LIU Ziliang[1], JIANG Zhikun[1], WEI Yingchun[1,2]

(1. College of Geoscience and Surveying Engineering, China University of Mining and Technology (Beijing), Beijing 100083, China; 2. State Key Laboratory for Fine Exploration and Intelligent Development of Coal Resources, China University of Mining and Technology (Beijing), Beijing 100083, China)

Abstract: During coalbed methane (CBM) production, coal fines within the reservoir can migrate, potentially blocking pore throats and resulting in a significant reduction in reservoir permeability. This process adversely affects the final CBM yield. To investigate the influence of coal fines migration on the porosity and permeability of cataclastic coal reservoirs, this study focuses on the processes of fines initiation, migration, and deposition within reservoir channels. The pore size distribution characteristics of cataclastic coal were analyzed using low-field nuclear magnetic resonance and low-temperature liquid nitrogen adsorption experiments. Subsequently, a three-dimensional pore network model was constructed, and a numerical model for coal fines migration and deposition in pore throat channels was developed. By integrating with an existing mechanical model for coal fines initiation and a probabilistic model for particle deposition and throat blockage, the Monte Carlo method was used to simulate the migration and blockage of coal fines within reservoir pores. A numerical simulation program written in Python was developed to simulate coal fines migration within the pore network of the cataclastic coal matrix. The variations in porosity and permeability of the reservoir during coal fines migration, as well as the influence of this migration, were discussed. The analysis revealed the internal mechanisms by which pressure difference and coal fines particle size

收稿日期：2024-09-19。
第一作者简介：石慧（2001—），女，在读硕士研究生，从事煤层气开发地质研究。地址：北京市海淀区学院路丁11号，邮政编码：100083。E-mail：shih_forward@163.com
通信作者简介：魏迎春（1977—），女，博士，教授，主要从事煤与煤系矿产资源地质勘探与开发方面的教学和科研工作。地址：北京市海淀区学院路丁11号，邮政编码：100083。E-mail：wyc@cumtb.edu.cn
基金项目：国家自然科学基金项目“不同类型构造煤储层中煤粉运移规律及其储层意义”（41972174）；国家自然科学基金项目“惰质组与镜质组大分子结构演化差异性及其动力学机制”（42042197）。

influenced coal fines output and model permeability. Both factors were significant, and their interactions were complicated. Specifically, the particle size of coal fines directly affected their migration, deposition, and output characteristics under different hydrodynamic conditions. Under low pressure difference and low flow velocity, large coal fines particles were difficult to mobilize and initiate migration. In contrast, under high pressure difference and high flow velocity, these particles became mobile but were more likely to block effective pores, resulting in a sharp decline in permeability. In addition, an increase in pressure difference had dual effects. It promoted coal fines output but also accelerated permeability decline rate. As the displacement pressure difference increased, the deposition location of coal fines shifted toward the outlet end, accompanied by a higher proportion of small throats. When the coal fines particle size was constant and smaller than the throat radius, a displacement pressure threshold was observed. On either side of this threshold, the relationship between the permeability decline rate and the displacement pressure showed distinct trends. During the drainage and depressurization stages of actual CBM production, the output characteristics and particle size distribution of coal fines served as important indicators for evaluating production efficiency and reservoir permeability changes. As drainage intensity gradually increased, the output intensity of coal fines experienced an initial slow growth followed by a rapid decline. Simultaneously, the particle size distribution of the produced coal fines reached its widest range, encompassing sizes from small to large, particularly during the initial drainage stage. When the drainage intensity was low, only small coal fines particles were mobilized and produced by fluid flow. To further investigate this, numerical simulations were conducted to replicate low drainage intensity conditions by setting a low pressure difference. The simulation results indicated that under low flow rates, small coal fines could indeed migrate and be produced, accompanied by a relatively gentle decline in reservoir permeability. These results were consistent with field observations under low drainage intensity, confirming the accuracy and reliability of the numerical simulation in predicting coal fines migration behavior. Furthermore, the numerical simulation results were compared with those from physical simulation experiments on coal fines migration. The model simulation results showed that as drainage continued, large coal fines particles settled preferentially within the pores. The deposition of these large particles formed channel barriers, blocking pore throats and significantly reducing permeability. Simultaneously, the deposition probability of small coal fines also increased rapidly. This made subsequent migration and production of coal fines increasingly difficult, resulting in a rapid decrease in coal fines production over time. In addition, physical simulation experiments of coal fines migration in cataclastic coal reservoirs provided valuable reference data. The experimental results showed that the permeability decrease of coal samples primarily occurred during the early stage of water flooding, and a higher fracture density corresponded to a higher average permeability. Pores and fissures with diameters greater than 1 000 nm served as the main channels for coal fines migration and blockage. The migrating coal fines further reduced permeability by plugging connected pores larger than 10 000 nm. These findings were consistent with the numerical simulation results, further confirming the alignment between permeability evolution and coal fines production during migration in cataclastic coal reservoirs. In simulations, high drainage intensity was simulated by setting a high pressure difference. When large coal fines were introduced, their deposition locations shifted compared with those under low pressure differences. Also, fines output decreased, and deposition became concentrated near the outlet end. When small coal fines were introduced, fines output increased significantly, and the permeability reduction was less severe than that caused by large coal fines. Overall, the model simulation results were consistent with coal fines output observed in actual production under increased drainage intensity. The numerical simulation results indicated that larger coal fines particles led to more concentrated deposition and blockage near the inlet end, with a smaller overall deposition range. Under low pressure difference, coal fines deposition was mainly concentrated near the inlet end. As the pressure difference increased, the deposition locations of coal fines shifted closer to the outlet end, and the deposition range expanded. In visual physical simulations of coal fines migration within fractures, the deposition area gradually decreased from the inlet toward both ends along and perpendicular to the main migration direction. In summary, the numerical simulation results were consistent with the permeability changes and coal fines deposition patterns observed during coal fines migration in physical simulation experiments.

Keywords: coalbed methane; cataclastic coal; coal fines migration; porosity and permeability; coal fines particle size; numerical simulation

中国构造煤发育[1],受工程扰动,导致煤层气开发中不同程度的煤粉产出,影响排采效率[2-4]。煤粉产出受流速、驱替压力及煤体结构等多种因素影响[5-11]。煤粉在流体携带下在储层孔裂隙中启动、运移、聚集沉积滞留于储层通道中,降低煤储层渗透率;其重新启动与排出能疏通通道,提高渗透率[12-15]。

当前对碎裂煤储层孔裂隙中煤粉的运移及沉降堵塞机制探讨较浅,利用CFD等数值模拟软件与流体力学方法[16-17],可直观分析煤粉质量浓度、流速及粒径对其运移的影响。前人将煤粉的流动机理分为产生、运移、和沉降3个阶段。当流速增大到煤粉由静态全部转化为动态时,水流剥蚀孔隙壁面,产生新煤粉[13-15]。当流速降低至煤粉临界沉积速率时,煤粉将停止运移而沉积[5]。煤粉沉降堵塞后聚团形成更大粒径的煤粉,难以再次启动运移[13-15]。针对煤粉在储层通道中启动、运移和沉积滞留过程,利用低场核磁共振和低温液氮吸附分析碎

裂煤孔径分布特征,建立三维孔隙网络模型。结合前人煤粉启动的力学模型和颗粒在喉道中的沉积堵塞概率模型,利用蒙特卡洛法模拟煤粉在储层孔隙中的运移和堵塞情况,利用python程序实现模拟过程,探讨排水降压单相流条件下,煤粉在碎裂煤储层大孔中的运移沉降规律。

1 煤粉启动—运移—堵塞理论模型

1.1 煤粉启动受力分析

碎裂煤由煤基质和裂缝组成,基质孔隙可视为孔隙-喉道网络。前人通过物理模拟实验得到:碎裂煤样中微孔>大孔>小孔>中孔,孔隙类型以狭缝型为主,喉道和裂缝之间的连通性较好,是煤粉的主要运移通道[18]。假设煤粉颗粒滚动启动,对单相流条件下碎裂煤喉道中的煤粉受力分析,有层流体对煤粉的拖拽力F_d、举升力F_l、煤粉与煤基质孔喉通道之间的黏附力合力,忽略煤粉重力,层流条件下圆管型通道内流体对煤粉的拖拽力和举升力可用下式表示[19-20]:

$$F_d = 1.700\,9 \times 6\pi\mu r^2\left[\frac{\Delta p}{2\mu L}(R-2r)\right] \tag{1}$$

$$F_l = 81.2\sqrt{\rho\mu}\,r^3\left[\frac{\Delta p}{2\mu L}(R-2r)\right]^{1.5} \tag{2}$$

式中:F_d为拖拽力,单位N;F_l为举升力,单位N;μ为流体绝对黏度,单位Pa·s;r为煤粉颗粒半径,单位m;ρ为流体密度,单位kg/m^3;Δp为通道两端压差,单位Pa;L为通道长度,单位m;R为通道半径,单位m。

煤粉与煤基质孔喉通道之间的黏附力合力为DLVO力(双电层斥力和范德华引力)和非DLVO力(伯恩斥力和lewis酸碱相互作用力),其合力可用总位能对距离求导得到[21]:

$$F_a = \frac{\partial \Phi_a}{\partial h} = \frac{\partial(\Phi_{EDL} + \Phi_{LVD} + \Phi_{BR} + \Phi_{AB})}{\partial h} \tag{3}$$

式中:F_a为黏附力合力,单位N;Φ_a为黏附力合力总位能,单位J;Φ_{EDL}为双电层斥力位能,单位J;Φ_{LVD}为Lifshitz-van Der Waals引力位能,单位J;Φ_{BR}为伯恩斥力位能,单位J;Φ_{AB}为lewis酸碱相互作用力位能,单位J;h为煤粉颗粒与喉道间的距离,单位m。

根据JKR接触理论,煤粉与基质表面间的接触半径以及力矩平衡公式如下[22]:

$$a = \left[3(F_a - F_l)r\left(\frac{1-v_1^2}{E_1} + \frac{1-v_2^2}{E_2}\right)\right]^{1/3} \tag{4}$$

$$F_d L_n = (F_a - F_l)a \tag{5}$$

式中:a为接触半径,单位m;L_n为阻力杠杆臂,单位m;E_1为裂缝面的杨氏模量,单位Pa;E_2为煤粉的杨氏模量,单位Pa;v_1为裂缝面的泊松比;v_2为煤粉的泊松比。

假设煤粉为有机质颗粒,驱替流体采用去离子水,水密度为0.997 g/cm^3,水黏度为0.895×10^{-3} Pa·s,K为煤粉颗粒和接触面的复合杨氏模量,其值为4.853×10^{-10} Pa,代入电荷参数[19]计算得到黏附力合力为0.143 4r J/m^2。将其带入式(1)—式(4),再带入式(5)得到有机质煤粉颗粒在低雷诺数单相层流中的启动临界速度[23]为:

$$v_0 = 2.989\,3 \times 10^{-4} \times \frac{(r)^{2/3}}{2(R-r)} \tag{6}$$

式中:v_0为煤粉启动的临界速度,单位m/s。

1.2 煤粉运移—堵塞喉道理论模型

颗粒在孔隙网络中的传输受孔隙空间的几何形态和流体动力学影响。通过受力与流体力学分析确定煤粉在喉道运移轨迹及时间,复杂网格中计算繁琐,因此,采用蒙特卡洛法,视煤粉运移为一个按照某些物理规则加权的随机概率。当判断煤粉的流动轨迹时,采用流动偏置概率,基于流量或注水压力来计算其随机性。其流动偏置概率可用下式表示:

$$P_k = \frac{q_k}{\sum_{z-1}^{i=1} q_i} \tag{7}$$

式中:P_k为流动偏置概率;q_k为第k个通道的流量,单位m^3/s;i为第i个通道;z为通道总个数;q_i为第i个通道流量,单位m^3/s。

若煤粉流向孔径小于自身半径的孔隙,会被拦截捕获,并改变流体的压力分布;若流向孔径大于自身半径的孔隙,利用颗粒通过比自身大的孔隙的捕获概率[17]:

$$P = 4\left[\left(\frac{\theta r}{R_0}\right)^2 - \left(\frac{\theta r}{R_0}\right)^3\right] + \left(\frac{\theta r}{R_0}\right)^4 \tag{8}$$

式中:P为捕获概率;R_0为初始喉道半径,单位m;θ为一个集总参数,受到流体速度、离子强度、pH值、流体性质、颗粒密度等性质的影响。

REGE等[24]进一步提出了θ的关系式:

$$\theta = \theta_0 \exp\left(-\frac{v}{v_0}\right) \tag{9}$$

式中:θ_0为常数,根据实验确定;v为流体流速,单位m/s。

煤粉颗粒沉积后会改变流体路径,导致喉道两端压力将发生变化,因此,颗粒沉积后等效的喉道有效半径为[17]:

$$\frac{1}{R_{new}^4} = \frac{1}{R_0^4} + 0.187\,5\frac{a}{L}\left[1-\left(1-\frac{a}{R_0}\right)^2\right]^2 K_1 \tag{10}$$

$$K_1=\frac{1-(2/3)(r/R_0)^2-0.202(r/R_0)^5}{1-2.1(r/R_0)+2.09(r/R_0)^3-1.71(r/R_0)^5+0.73(r/R_0)^6} \tag{11}$$

式中：R_{new}为等效的喉道有效半径，单位m。

根据上述公式，颗粒半径越大沉积后的有效半径越小，使得流动阻力变大、渗流能力减弱及渗透率下降。将碎裂煤孔径分布范围代入式(6)和式(8)验证模型的准确性并设置不同的颗粒半径参数，得到煤粉颗粒沉降概率随着喉道半径变化的曲线(图1)。

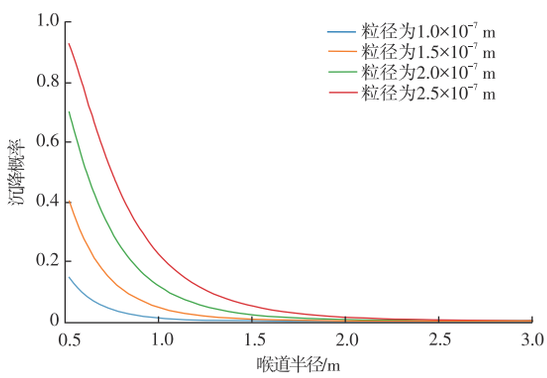

图1　不同粒径煤粉颗粒沉降概率随着喉道半径变化的规律

Fig. 1　Variations in deposition probability of coal fines with throat radius for different particle sizes

由图1可知：随喉道半径增大，煤粉沉降概率呈指数变小，即喉道半径的大小是影响煤粉运移和堵塞的关键。煤粉沉降概率随着颗粒半径的增大而增大，大粒径煤粉更易沉降堵塞裂隙。根据式(10)可知大粒径煤粉沉降导致有效渗流空间减小更多，增大了后续煤粉沉降概率。因此，大粒径煤粉运移迅速缩减储层渗流空间及渗透率。

2　碎裂煤孔隙网络模型的构建

2.1　孔隙网络模型建立

构建粒子的运移沉降和孔隙网络模型，模拟颗粒在孔隙网络中的运移沉积。由多孔介质的相互链接性简化孔隙结构，用OpenPNM(是一个用Python语言编写的用于建立孔隙网络模型的开源软件包)建立三维立方体孔隙网络模型和体心立方网络模型，网格节点数量设置为10×10×10，网格间距为1×10^{-5} m，孔喉形状因子选择球形和圆柱形。基于韩城区碎裂煤的孔径分布，给网络中的孔隙和喉道进行赋值。根据碎裂煤的核磁图像，其孔径分布近似为对数正态分布，且物理模拟结果表明，基质中孔径大于1×10^{-6} m的大孔是煤粉运移和堵塞的主要通道[18]。因此，将OpenPNM中孔径分布设为对数正态分布，分布的中值设为$10^{-1.9}$ μm，其对数标准差设为0.34 μm，应用后得到的喉道半径分布如图2所示。

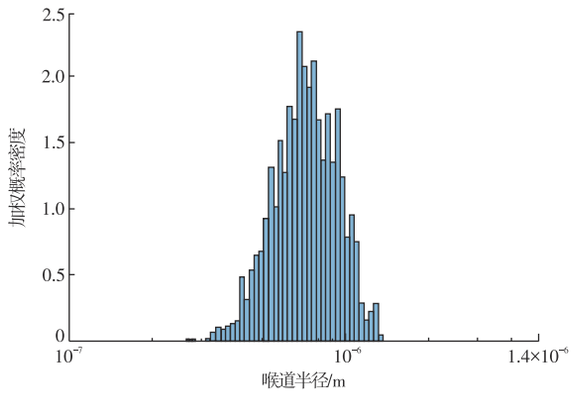

图2　初始模型的喉道半径分布

Fig. 2　Throat radius distribution in initial model

2.2　流体相参数以及主程序建立

为探究煤粉运移对碎裂煤孔渗的影响，基于煤粉运移沉降模型利用Python编程，模拟煤粉在孔喉通道中的运移沉降过程。驱替流体利用单相水流，采用达西定律计算渗透率，喉道流动阻力公式采用哈根-泊肃叶定律，流体流动及压力分布采用斯托克斯流动模拟。颗粒沉降概率、喉道有效半径计算和流动路径判断分别运用式(8)、式(10)和式(7)。将模型的左、右边界分别视为入口端、出口端，在模型入口端生成颗粒。当颗粒生成位置的流体速度大于煤粉启动的临界速度，煤粉启动运移。当煤粉运移到大于自身半径的喉道时，用式(8)计算该处的沉积捕获概率并判断其是否会被捕获，随后根据式(10)计算该处喉道捕获颗粒后的有效半径，再根据哈根-泊肃叶定律重新计算喉道流动阻力；当煤粉运移到小于自身半径的喉道时，会被捕获并堵塞喉道，增大流动阻力。当颗粒发生捕获后，重新模拟流体相并计算模型各处的流量和压力差。整个程序的框架如图3所示。

3　模拟计算结果及分析

3.1　粒径大小对煤粉运移以及孔渗的影响

为研究煤粉粒径对其运移规律及孔渗的影响，设粒径分别为0.10、0.15、0.20、0.25 μm，模拟单相流运移。图4a—图4d为驱替后喉道半径的分布变化，小粒径煤粉驱替后孔喉分布相比驱替前，半径在更小的10^{-7} m尺度上的喉道数量增加，随煤粉粒径增大，占比开始减小。图5a—图5d中红色线条代表颗粒沉积位置，主要在入

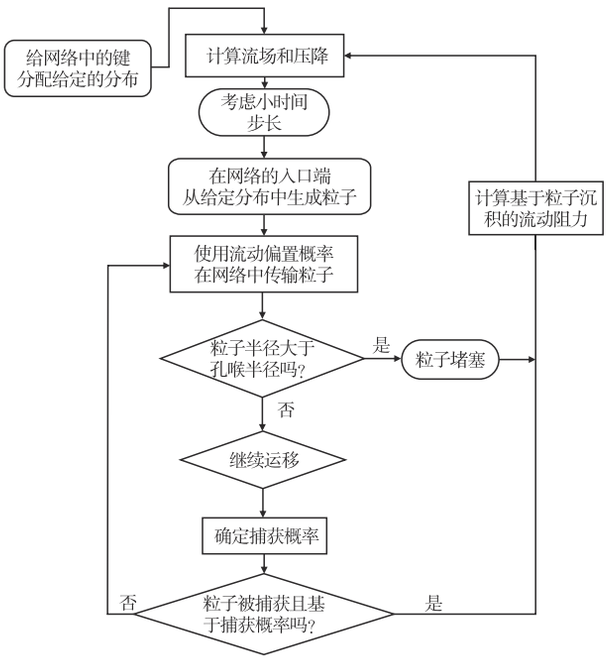

图3　驱替模拟流程

Fig. 3　Flowchart of displacement simulation

口端沉降，粒径越大，沉降越集中范围越小。前期颗粒沉降堵塞通道，后续的颗粒难以通过，沉降概率变大。粒径由小到大沉降煤粉颗粒量朝出口端方向减少。由式(10)可知小粒径颗粒有更大几率通过喉道，随粒径增大，颗粒沉降引起的有效半径减小较多，使后续颗粒通过的难度变高，故颗粒大多沉降在入口端，后续煤粉难以运移到基质其他位置沉降，故煤粉粒径越大基质孔径分布变化越小。

由图6a可知，不同粒径煤粉的渗透率下降速度和幅度不同，但整体趋势相似。煤粉主要在模型前中部沉降，堵塞渗流通道，导致渗透率下降，下降速度先快后慢。随着粒径增大，模型沉降概率及速度变高，导致渗流通道更快被堵塞及煤粉运移的有效通道被堵塞的速度变快，更快速地阻止了煤粉向其他渗流通道运移，即表现为粒径越大其下降速度达到拐点的时间越靠前。

3.2　压差大小对煤粉运移以及孔渗的影响

为研究压差对煤粉运移及孔渗的影响，设压差分别为5、10、15、20 MPa，模拟单相流运移。图4e—图4h为驱替后喉道半径的变化，驱替后喉道数量在半径为1×10^{-7} m尺度上显著增加，且随压差增大越显著。图5e—图5h中红色线条代表颗粒沉积位置，低压差时煤粉主要在入口端沉降，随压差增大，沉降位置向出口端扩展。

上述现象表明在驱替过程中压差直接影响煤粉颗粒运移，压差越大流速越大，则煤粉沉降概率越低。利用碎裂煤半径分布模拟非均质性，煤粉更易运移到更小喉道处沉降堵塞，沉降范围随压差增大而扩大，喉道半径分布趋向更小尺度。由图6b可知，不同压差条件下渗透率变化趋势不同。压差5 MPa时渗透率为阶梯式下降，而压差介于10～20 MPa条件下时渗透率近似一个曲线。因为数值模拟的初始状态不含煤粉，所以当模拟进行时煤粉启动—运移—沉降堵塞渗流通道，使渗透率整体呈下降趋势。结合煤粉颗粒的受力分析和启动模型，当压差为5 MPa时流速较低，大部分通道内的流速小于煤粉受力启动的临界速度，只有生成在少数流速较高的通道内的煤粉会发生运移然后沉降，因此，渗透率下降呈现阶梯式分布；当压差增至10 MPa时，多数通道内的流速超过煤粉的启动临界速度，大部分煤粉运移沉降堵塞有效渗流通道使渗透率下降；当压差增至20 MPa时，煤粉的沉降速度反而低于15 MPa条件下的，据式(8)和式(9)煤粉沉降概率会随着流速增大而降低，因此，当压差增大到一定程度，煤粉的沉降速度变慢，导致压差达到一定阈值后渗透率的下降速度开始减慢。

3.3　数值模拟与物理模拟实验结果相互验证

在模型程序中加入粒子产出的检测，通过检测运移到模型出口端上的颗粒数量模拟煤粉颗粒产出。在压差为10 MPa条件下生成0.15 μm和0.25 μm粒径的煤粉，模拟运行300 s得到煤粉累计产出量及渗透率变化情况(图7)。对比压差为5 MPa条件下可知，增大压差使煤粉产出量明显增大，减小压差渗透率下降的速度和幅度降低。如图8将纵坐标设为每隔10 s产出的煤粉颗粒数量，得到实时煤粉产出量，且产出颗粒数量随时间快速下降后稳定为较低数值。前人研究韩城区块煤粉产出特征发现[25]：初始排液时，低排水强度下只有部分小粒径煤粉运移产出。数值模拟中利用低压差模拟低排水强度，在较低的流速下，小粒径煤粉会运移产出，且渗透率下降速度较缓慢。压差为5 MPa时，设颗粒半径为0.25 μm，模型只有极少数位置有煤粉颗粒沉降，产出煤粉颗粒数量为0；设颗粒半径为0.15 μm，运行100 s后产出煤粉颗粒数量达到122个，其与实际生产中较低排水强度下的煤粉产出情况基本一致。

在实际生产中，可以增加排水强度使煤粉产出增多[25]。随着模拟排水进行，大粒径煤粉会优先在孔隙中沉降堵塞有效孔隙，使渗透率下降及小粒径煤粉沉降概率快速上升，表现为产出煤粉颗粒数量随时间快速下降。前人通过碎裂煤储层煤粉运移物理模拟实验表明：孔径大于1 000 nm的孔和裂隙是煤粉运移和堵塞的主要通道，煤粉通过运移堵塞孔径大于10 000 nm的连通孔隙导致渗透率降低[17]与数值模拟结果一致。用压力为10 MPa模拟高排水强度，当颗粒半径为0.25 μm，相较于5 MPa，煤粉的沉降

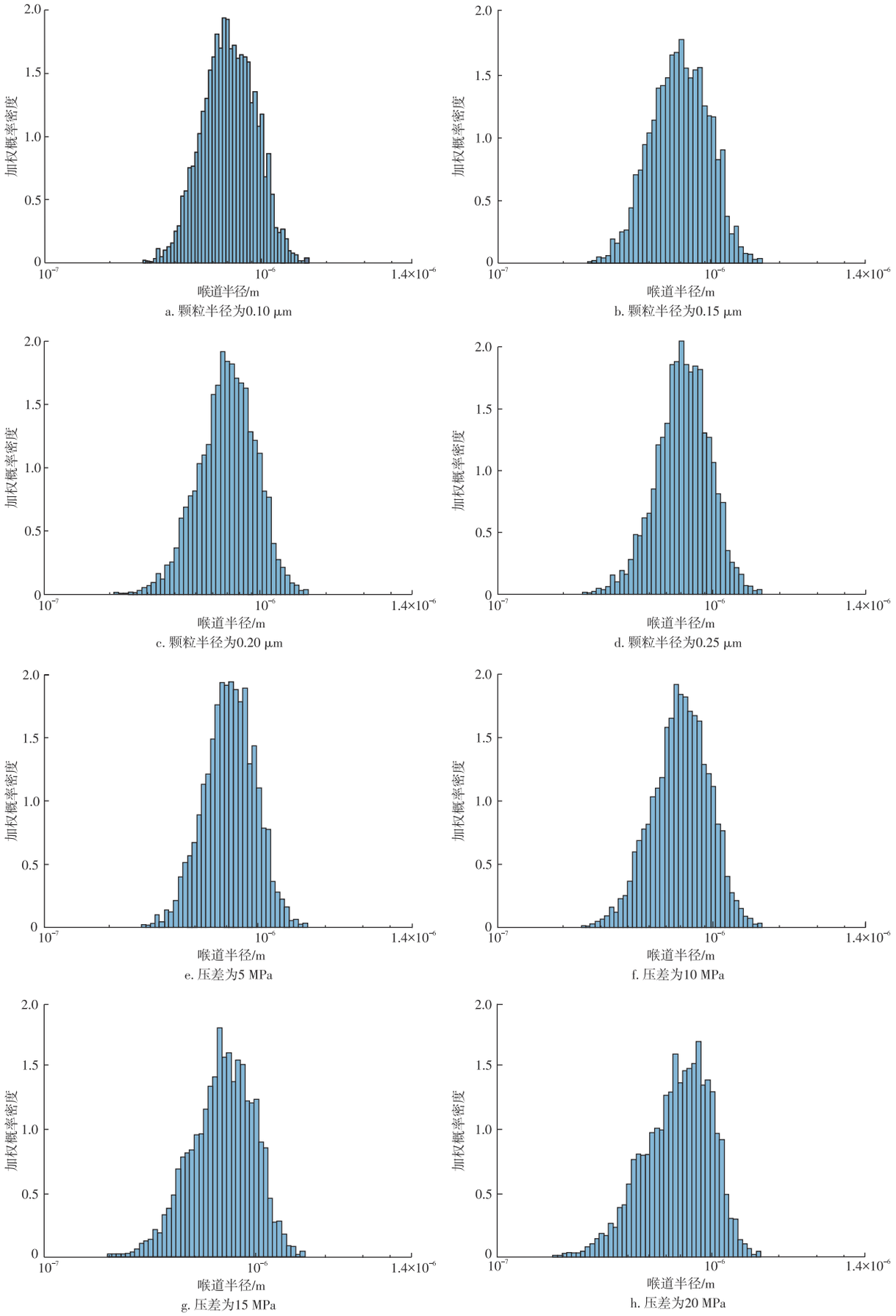

图4 不同粒径和不同压差条件下模型驱替后的喉道半径分布

Fig. 4 Throat radius distribution after displacement under different particle sizes and pressure differences

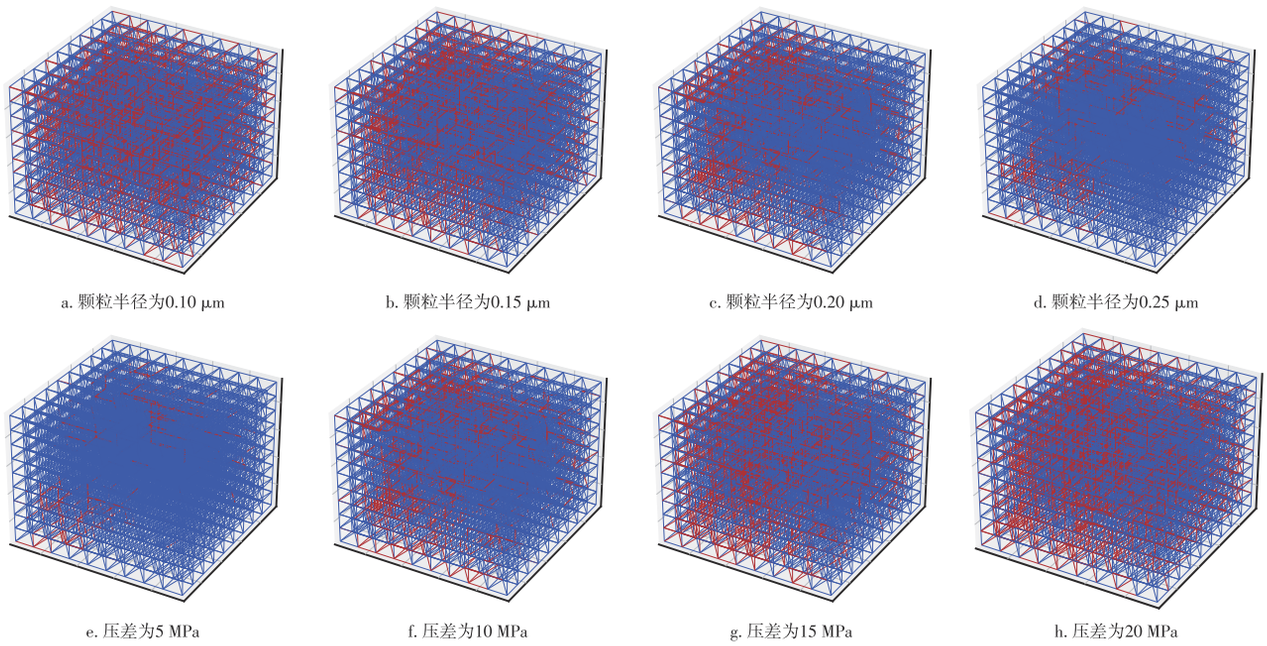

图5　不同粒径条件下和不同压差条件下模型驱替后的煤粉沉降位置

Fig. 5　Deposition locations of coal fines after displacement under different particle sizes and pressure differences

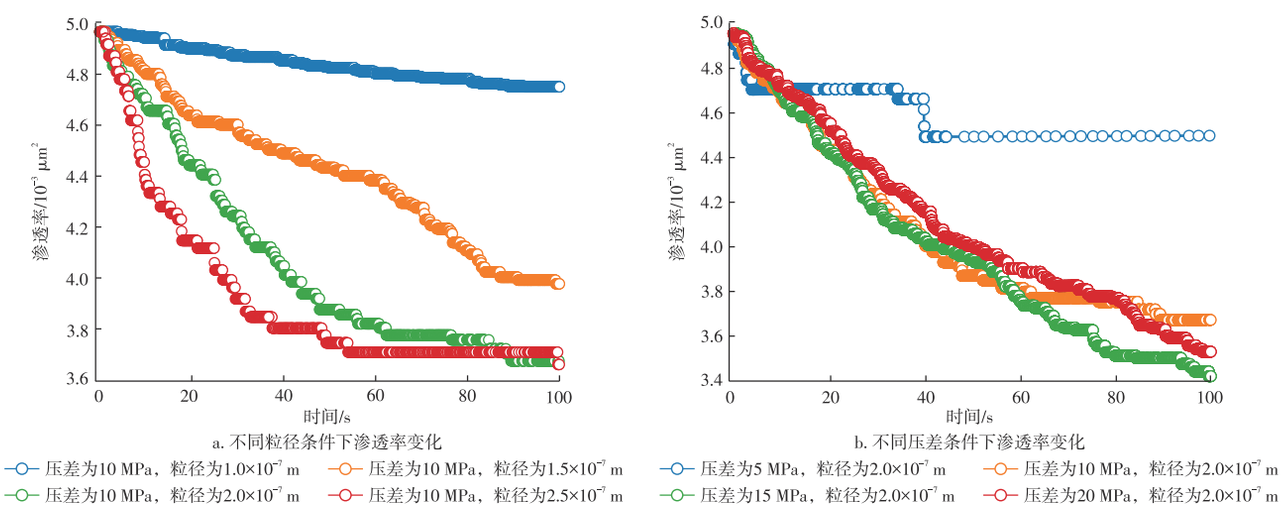

图6　不同粒径条件下和不同压差条件下模型的渗透率变化

Fig. 6　Permeability variations of model under different particle sizes and pressure differences

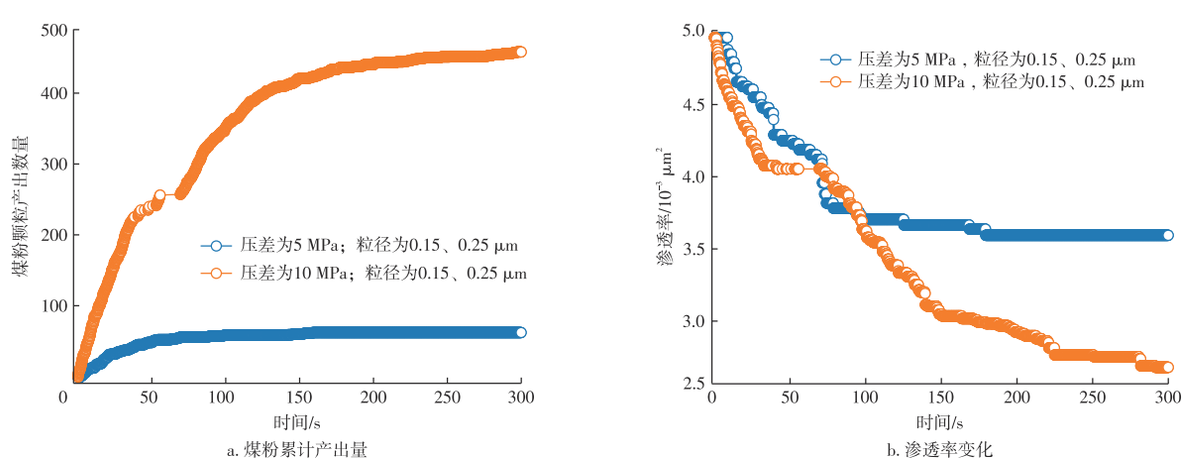

图7　不同压差条件下混合粒径模型的煤粉累计产出量和渗透率变化

Fig. 7　Cumulative production of coal fines and permeability variations of mixed-particle-size model under different pressure differences

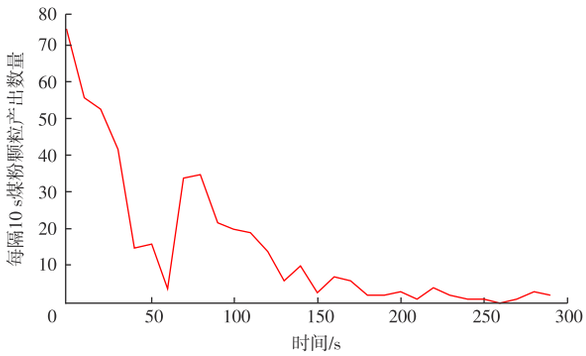

图8 混合粒径情况下的煤粉产出量随时间的变化

Fig. 8 Temporal variations in coal fines production under mixed particle sizes

位置增多，产出量减少，渗透率下降幅度为1.310×10^{-3} μm²；当颗粒半径为0.15 μm，煤粉的产出量明显增多，渗透率下降幅度缩小至0.987×10^{-3} μm²，与实际生产中增大排水强度后的煤粉产出情况一致。数值模拟显示，煤粉粒径增大使沉降堵塞更集中于入口端。低压差时，煤粉主要在入口端沉降；压差增大，沉降位置向出口端扩展，范围增大。前人在裂隙中模拟可视化的煤粉运移实验表明裂隙喉道由入口向垂直主运移方向的两端及主运移方向煤粉颗粒沉积面积逐渐减少[12]，与数值模拟结果一致。

4 结论

1）在压差一定的条件下，随着煤粉粒径增大，渗透率的下降幅度和下降速度增大。大粒径的煤粉颗粒更容易快速堵塞有效孔隙喉道，同时也会导致煤粉运移的有效通道被堵塞的速度变快。

2）在煤粉粒径不变且整体上粒径小于喉道半径的情况下，驱替压力存在一个阈值。当小于这个阈值时，增大驱替压力，渗透率的下降速度会增加；而大于这个阈值时，增大驱替压力，渗透率的下降速度会降低。

3）数值模拟实验结果表明：在压差较低、粒径较大的情况下，煤粉产出量较低，同时渗透率下降速度较慢、下降幅度更低，其与煤粉运移的物理模拟实验结果一致。

参 考 文 献

[1] 曹代勇, 袁远, 魏迎春, 等. 煤粉的成因机制-产出位置综合分类研究[J]. 中国煤炭地质, 2012, 24(1): 10-12.
CAO Daiyong, YUAN Yuan, WEI Yingchun, et al. Comprehensive classification study of coal fines genetic mechanism and origin site [J]. Coal Geology of China, 2012, 24(1): 10-12.

[2] 魏迎春, 曹代勇, 袁远, 等. 韩城区块煤层气井产出煤粉特征及主控因素[J]. 煤炭学报, 2013, 38(8): 1424-1429.
WEI Yingchun, CAO Daiyong, YUAN Yuan, et al. Characteristics and controlling factors of pulverized coal during coalbed methane drainage in Hancheng area[J]. Journal of China Coal Society, 2013, 38(8): 1424-1429.

[3] 魏迎春, 李超, 曹代勇, 等. 煤层气开发中煤粉产出机理及管控措施[J]. 煤田地质与勘探, 2018, 46(2): 68-73.
WEI Yingchun, LI Chao, CAO Daiyong, et al. The output mechanism and control measures of the pulverized coal in coalbed methane development[J]. Coal Geology & Exploration, 2018, 46(2): 68-73.

[4] 孟文辉, 张文, 王博洋, 等. 保德区块煤粉产出特征及其影响要素剖析[J]. 油气藏评价与开发, 2023, 13(4): 441-450.
MENG Wenhui, ZHANG Wen, WANG Boyang, et al. Analysis of characteristics of coal fine production and its influence factors in Baode block[J]. Petroleum Reservoir Evaluation and Development, 2023, 13(4): 441-450.

[5] 曹代勇, 姚征, 李小明, 等. 单相流驱替物理模拟实验的煤粉产出规律研究[J]. 煤炭学报, 2013, 38(4): 624-628.
CAO Daiyong, YAO Zheng, LI Xiaoming, et al. Rules of coal powder output under physical simulation experiments of single-phase water flow displacement[J]. Journal of China Coal Society, 2013, 38(4): 624-628.

[6] BAI T, CHEN Z, AMINOSSADATI S M, et al. Experimental investigation on the impact of coal fines generation and migration on coal permeability[J]. Journal of Petroleum Science & Engineering, 2017, 159: 257-266.

[7] HAN W, WANG Y, LI Y, et al. Coal fines migration, deposition, and output simulation during drainage stage in coalbed methane production[J]. Energy & Fuels, 2021, 35(6): 4901-4913.

[8] LIU Z, WEI Y, SHI X, et al. Experimental study on the influence of hydrochemical properties on the migration of coal fines containing kaolinite in propped fractures[J]. Energy & Fuels, 2023, 37(16): 12007-12017.

[9] YAO Z, CAO D, WEI Y, et al. Experimental analysis on the effect of tectonically deformed coal types on fines generation characteristics [J]. Journal of Petroleum Science & Engineering, 2016, 146: 350-359.

[10] WEI Y, LIU Z, XIONG X, et al. Experimental study of coal fines migration characteristics in reservoirs with diverse coal structures: Influence on reservoir behavior[J]. Gas Science and Engineering, 2024, 130: 205438.

[11] REN J G , SONG Z M, LI B, et al. Structure feature and evolution mechanism of pores in different metamorphism and deformation coals [J]. Fuel, 2021, 283: 119292.

[12] 魏迎春, 张琦, 刘子亮, 等. 裂隙中煤粉运移及解堵可视化物理模拟实验[J]. 煤炭学报, 2024, 49(3): 1488-1500.
WEI Yingchun, ZHANG Qi, LIU Ziliang, et al. Visual physical simulation experiment of coal fines migration and blockage removal in fractures[J]. Journal of China Coal Society, 2024, 49(3): 1488-1500.

[13] PENG X, ZHU S, YOU Z, et al. Numerical simulation study of fines migration impacts on an early water drainage period in undersaturated coal seam gas reservoirs[J]. Geofluids, 2019, (1): 5723694.

[14] 张健, 朱苏阳, 彭小龙, 等. 煤层气-水-固三相流动模型与数值模拟研究[J]. 中国海上油气, 2022, 34(1): 117-127.
ZHANG Jian, ZHU Suyang, PENG Xiaolong, et al. Tri-phase flow model of coalbed methane-water-solid and numerical simulation

study[J]. China Offshore Oil and Gas, 2022, 34(1): 117-127.

[15] 杨龙, 张艺钟, 徐亚飞, 等. 一种修正的煤层气藏地层压力与含水饱和度的关系模型[J]. 断块油气田, 2023, 30(2): 294-300.
YANG Long, ZHANG Yizhong, XU Yafei, et al. A modified model for the relationship between formation pressure and water saturation in coalbed methane reservoirs[J]. Fault-Block Oil & Gas Field, 2023, 30(2): 294-300.

[16] ZHU S Y, PENG X L, DU Z M, et al. Modeling of coal fine migration during CBM production in high-rank coal[J]. Transport in Porous Media, 2017, 118(1): 65-83.

[17] 任石磊, 韩飞鹏, 谢斌, 等. 基于三维CFD-DEM的多孔介质流场数值模拟[J]. 应用数学和力学, 2017, 38(10): 1093-1102.
REN Shilei, HAN Feipeng, XIE Bin, et al. Numerical simulation of flow fields in porous media based on the 3D CFD-DEM[J]. Applied Mathematics and Mechanics, 2017, 38(10): 1093-1102.

[18] XIE T C, WEI Y C, LIU Z L, et al. Experimental investigation on the impact of coal fines migration on pores and permeability of cataclastic coal[J]. ACS Omega, 2023, 8(34): 31246-31255.

[19] 皇凡生, 康毅力, 李相臣, 等. 单相水流诱发裂缝内煤粉启动机理与防控对策[J]. 石油学报, 2017, 38(8): 947-954.
HUANG Fansheng, KANG Yili, LI Xiangchen, et al. Incipient motion mechanisms and control measures of coal fines during single-phase water flow in coalbed fractures[J]. Acta Petrolei Sinica, 2017, 38(8): 947-954.

[20] O'NEILL M E. A sphere in contact with a plane wall in a slow linear shear flow[J]. Chemical Engineering Science, 1968, 23(11): 1293-1298.

[21] VAN OSS C J, CHAUDHURY M K, GOOD R J. Interfacial Lifshitz-van der Waals and polar interactions in macroscopic systems[J]. Chemical Reviews, 1988, 88(6): 927-941.

[22] BERGENDAHL J, GRASSO D. Prediction of colloid detachment in a model porous media: Hydrodynamics[J]. Chemical Engineering Science, 2000, 55(9): 1523-1532.

[23] MACKIE R I, HORNE R M W, JARVIS R J. Dynamic modeling of deep-bed filtration[J]. Aiche Journal, 1987, 33(11): 1761-1775.

[24] REGE S D, FOGLER H S. A network model for deep bed filtration of solid particles and emulsion drops[J]. Aiche Journal, 1988, 34(11): 1761-1772.

[25] 魏迎春, 张傲翔, 姚征, 等. 韩城区块煤层气排采中煤粉产出规律研究[J]. 煤炭科学技术, 2014, 42(2): 85-89.
WEI Yingchun, ZHANG Aoxiang, YAO Zheng, et al. Research on output laws of pulverized coal during coalbed methane drainage in Hancheng Block[J]. Coal Science and Technology, 2014, 42(2): 85-89.

(编辑 李青)